BIOCHEMISTRY
including biophysical chemistry & molecular biology
Article

Biochemistry **2010,** *49,* 4383–4394 4383
DOI: 10.1021/bi901764m

Scherffelia dubia Centrin Exhibits a Specific Mechanism for Ca^{2+}-Controlled Target Binding†

Laura Radu,‡,§ Isabelle Durussel,∥ Liliane Assairi,*,‡,§ Yves Blouquit,‡,§ Simona Miron,‡,§ Jos A. Cox,*,∥ and Constantin T. Craescu‡,§,⊥

‡*Institut Curie Centre de Recherche, Centre Universitaire Paris-Sud, 91405 Orsay Cedex, France,* §*INSERM U759, Centre Universitaire Paris-Sud, 91405 Orsay Cedex, France, and* ∥*Department of Biochemistry, University of Geneva, Geneva 4, Switzerland* ⊥*Deceased.*

Received October 13, 2009; Revised Manuscript Received April 21, 2010

ABSTRACT: Centrins are calcium binding proteins that belong to the EF-hand (or calmodulin) superfamily, which are highly conserved among eukaryotes. Herein, we report the molecular features and binding properties of the green alga *Scherffelia dubia* centrin (SdCen), a member of the *Chlamydomonas reinhardtii* centrin (CrCen) subfamily. The Ca^{2+} binding capacity of SdCen and its isolated N- and C-terminal domains (N-SdCen and C-SdCen, respectively) was investigated using flow dialysis and isothermal titration calorimetry. In contrast with human centrin 1 and 2 (from the same subfamily), but like CrCen, SdCen exhibits three physiologically significant Ca^{2+} binding sites, two in the N-terminal domain and one in the C-terminal domain. Mg^{2+} ions could compete with Ca^{2+} in one of the N-terminal sites. When Ca^{2+} binds, the N-terminal domain becomes more stable and exposes a significant hydrophobic surface that binds hydrophobic fluorescent probes. The Ca^{2+} binding properties and the metal ion-induced structural changes in the C-terminal domain are comparable to those of human centrins. We used isothermal titration calorimetry to quantify the binding of SdCen, N-SdCen, and C-SdCen to three types of natural target peptides, derived from the human XPC protein (P17-XPC), the human Sfi1 protein (R17-hSfi1), and the yeast Kar1 protein (P19-Kar1). The three peptides possess the complete (P17-XPC and R17-hSfi1) or partial (P19-Kar1) centrin binding motif ($W^1L^4L^8$). The integral SdCen exhibits two binding sites for each target peptide, with distinct affinities for each site and each peptide. The high-affinity peptide binding site corresponds to the C-terminal domain of SdCen and displays binding constants and the poor Ca^{2+} sensitivities similar to those observed for human centrins. The low-affinity site constituted by the N-terminal domain is active only in the presence of Ca^{2+}. The thermodynamic binding parameters suggest that the C-terminal domain of SdCen may be constitutively bound to a target, while the N-terminal domain could bind a target only after a Ca^{2+} signal. SdCen is also able to interact with calmodulin binding peptides ($W^1F^5V^8F^{14}$ motif) with a 1:1 stoichiometry, whereas the isolated N- and C-terminal domains have a much lower affinity. These data suggest particular molecular mechanisms used by SdCen (and probably by other algal centrins) to respond to cellular Ca^{2+} signals.

Centrins are acidic Ca^{2+} binding proteins of the EF-hand superfamily, well conserved in the eukaryotic kingdom (*1*, *2*). Centrins were first identified in unicellular green algae, such as *Tatraselmis striata* (*3*) and *Chlamydomonas reinhardtii* (*4*, *5*), as components of the basal bodies-associated, Ca^{2+}-sensitive contracting fibers. The capacity of the centrin-based filaments to contract with an increase in Ca^{2+} concentration, even in the absence of ATP (*3*), suggested that centrins are responsible for Ca^{2+}-dependent motility processes, at least in ciliated or flagellate cells. Flagellar excision, as a response to adverse environmental conditions in algae, is also dependent on centrin filaments and seems to be regulated by the intracellular Ca^{2+} concentration (*5*).

Centrins have since been found to be ubiquitous proteins in many other eukaryotic species, including higher plants (*6*), yeast (*7*), invertebrates (*8*), and humans (*9*, *10*) (see ref *11* for a review). The protein is concentrated in the microtubule-organizing centers (MTOCs),[1] functionally similar to basal bodies, which are named spindle pole body (SPB) in yeast and centrosome in higher eukaryotes. Accumulation of proteomic data for various species allowed the establishment of a phylogenic tree of the centrin family that has four main subfamilies (*11*, *12*). *C. reinhardtii* centrin (CrCen) is the prototype for the largest subfamily, which comprises also human centrins HsCen1 and HsCen2. Human centrin 3 (HsCen3) and yeast centrin (Cdc31) form the next subfamily,

†This work was supported by the Centre National de la Recherche Scientifique, the Institut National de la Santé et de la Recherche Médicale, the Institut Curie, and a grant from the Swiss National Science Foundation (3100AQ-108215/1). L.R. was a recipient of a Ph.D. grant from the Institut Curie.

*To whom correspondence should be addressed. L.A.: Institut Curie and INSERM U759, Centre Universitaire Paris-Sud, 91405 Orsay Cedex, France; telephone, 33(0)169863178; fax, 33(0)169075327; e-mail, liliane.assairi@curie.u-psud.fr. J.A.C.: Department of Biochemistry, University of Geneva, Geneva 4, Switzerland; e-mail, Jos.Cox@unige.ch.

[1]Abbreviations: SdCen, *Scherffelia dubia* centrin; N-SdCen, N-terminal domain (M1−M93) of SdCen; C-SdCen, C-terminal domain (M93−F168) of SdCen; HsCen1−HsCen3, human centrin isoforms 1−3, respectively; CrCen, *C. reinhardtii* centrin; CaM, calmodulin; ME, melittin; TNS, 2-*p*-toluidinylnaphthalene 6-sulfonate; P19-Kar1, K237−K255 peptide of the yeast Kar1 protein; P17-XPC, N847−R863 peptide from the human XPC protein; R17-Sfi1, R641−T660 peptide of human protein hSfi1; skMLCK, K566−S587 peptide derived from human skeletal muscle myosin light chain kinase protein; MTOC, microtubule-organizing center; SPB, spindle pole body; ITC, isothermal titration calorimetry.

Published on Web 04/21/2010

while plant and paramecium centrins define the two other subfamilies.

The functional significance and molecular mechanism of centrin-mediated motility are actually not known. However, a clear sign of progress was the discovery in yeast and human cells of a centrin target protein named Sfi1, containing a large number of similar sequence motifs, each being able to bind a centrin molecule independently (*13*). The centrin−Sfi1 interaction studies (*13*, *14*) showed that the binding affinity is moderately increased (~20-fold) by Ca^{2+}, suggesting that the two proteins are constitutively bound. However, the mechanism of Ca^{2+}-controlled contraction of centrin−Sfi1 complexes is not known (*14*, *15*) and requires additional experimental investigation.

The presence of centrins in the centrosome is related to another functional role, the regulation of the MTOC duplication and separation during the cell cycle. It was clearly demonstrated in several eukaryotic species that the absence or a nonfunctional centrin induces a failure of MTOC duplication and defects in cellular mitosis (*16*−*20*). Nothing is known about an eventual centrin-mediated role of Ca^{2+} in this process.

New centrin implications are currently being discovered in various cellular processes, including nucleotide excision repair (*21*), the light transduction cascade in photoreceptor cells (*22*), the ciliary voltage-gated Ca^{2+} channel in *Paramecium* (*23*), axonemal chemotaxis in *Tetrahymena* (*24*), and the nuclear mRNA export machinery in yeast (*25*, *26*).

Centrin molecules (~20 kDa) consist of two relatively independent EF-hand domains, each one including two EF-hand motifs. The N-terminal domain of centrins contains a highly variable and unstructured fragment of 20−25 amino acids and exhibits more variable Ca^{2+} binding properties relative to the C-terminal domain. Each molecule possesses four potential Ca^{2+} binding sites (I−IV), but because of amino acid substitutions in the binding loop sequence or in the adjacent helices, the affinity and specificity for Ca^{2+} ion may vary from one species to another. For instance, HsCen1 and HsCen2 have a moderate-affinity (K_d of 10 μM for site IV) and a low-affinity (K_d of > 100 μM for site III) Ca^{2+} binding site, while the N-terminal domain has nonphysiological (K_d > 1 mM) ion binding sites (*27*−*29*). HsCen3 displays one high-affinity Ca^{2+}/Mg^{2+}-mixed site, which likely sits in EF-hand I, and two low-affinity Ca^{2+}-specific sites (*30*). Green algal CrCen binds three Ca^{2+} ions per monomer with submillimolar dissociation constants, displaying higher affinity for the two N-terminal sites (1−10 μM) and a distinctly lower affinity (~100 μM) for the C-terminal site (*31*).

Understanding of centrin functions, and particularly the Ca^{2+} dependence, requires a detailed description of the molecular and structural properties of the isolated proteins and of their interactions with relevant cellular targets. Algal centrins exhibit specific properties as compared to centrins from the same phylogenic subfamily such as human centrin 1 and 2. In addition, cellular investigations of green algae (*Chlamydomonas* and *Tetraselmis*) (*32*, *33*) have documented the participation of centrins in a network of Ca^{2+}-sensitive fibers connecting the basal bodies among them and with the nucleus. *Scherffelia dubia* centrin was reported to polymerize in a Ca^{2+}-dependent manner and to form a filamentous network (*39*). We therefore initiated a molecular and thermodynamic study that aimed to determine the detailed Ca^{2+} binding parameters and Ca^{2+}-dependent functional properties of the algal *S. dubia* centrin (SdCen). Our data show that SdCen and CrCen share a unique molecular property, the capacity of the N-terminal domain to bind two Ca^{2+} ions with high affinity and to change its conformation upon Ca^{2+} binding. Consequently, the N-terminal domain could bind target motifs in a strict Ca^{2+}-dependent manner. At low Ca^{2+} concentrations, only the C-terminal domain may bind a target molecule, while in the presence of a Ca^{2+} signal, the N-terminal domain can also bind the target and the whole SdCen protein may interact simultaneously with two protein targets. These experimental observations emphasize a distinct functional mode of SdCen as compared to that of centrins from the same subfamily (HsCen1 and HsCen2) or centrins from the Cdc31 subfamily. Similar molecular properties of SdCen and CrCen suggest that this functional feature could be common to all the algal centrins. This hypothesis is supported by sequence comparison of centrins from algae and nonplant organisms, which also suggests that the sequence signature of the plant and algae centrins is mainly localized in the second EF-hand.

MATERIALS AND METHODS

Materials. Melittin (ME) was purchased and further purified as described previously (*34*). Peptides P17-XPC, P19-Kar1, R17-hSfi1 (corresponding to the R641−T660 sequence of human Sfi1 protein), and skMLCK were purchased from Biofidal (Vaulx-en-Velin, France) and Hybio (Shenzhen, China). All the peptides are acetylated at the N-terminus and amidated at the C-terminus. Purity was greater than 95%, as assessed by high-pressure liquid chromatography analysis. The primers were purchased from Eurogentec.

Cloning, Expression, and Purification of the Proteins. The *S. dubia* centrin (SdCen) coding sequence was amplified from a plasmid containing the centrin gene (kindly provided by M. Melkonian, University of Köln, Cologne, Germany), according to the polymerase chain reaction (PCR) method by using the Vent or Phusion DNA polymerase, the dNTPs, and the flanking 5′- and 3′-primers (5′-GGAATTCCATATGAGCTACAGGA-AGGCTGCC-3′ and 5′-GGCGCTCGAGTCAGAACAGTG-ACGTCTTCTTCATG-3′, respectively). The PCR products were inserted at the NdeI and XhoI restriction sites of the pET24a expression vector using T4 DNA ligase. This recombinant plasmid was used as a template for PCR amplification of the N-terminal domain (Met1−Met93) of SdCen (or N-SdCen) using the 3′-primer (5′-CGGCGCTCGAGTCACATCTTGGCGGTCATCATCTG-3′) and of the C-terminal domain (Met93−Phe168) of SdCen (or C-SdCen) using the 5′-primer (5′-GGAATTCCATATGGGC-GAGCGCGACTCCC-3′). The resulting plasmids encoding either SdCen, N-SdCen, or C-SdCen were used to transform *Escherichia coli* strain NM554, and the clones obtained were sequenced to verify their integrity and finally used to transform *E. coli* strain Bl21(DE3)/pDIA17 for further expression of the protein. For overproduction of SdCen and its two domains, the transformants containing the specific plasmid were grown at 37 °C in 2YT medium (Difco) in the presence of chloramphenicol (30 μg/mL) and kanamycin (70 μg/mL). When the absorbance reached 1.5 at 600 nm, the production of the protein was induced by addition of 1 mM isopropyl β-D-1-thiogalactopyranoside, and the growth was continued for an additional 3 h at 37 °C. The cells were then pelleted by centrifugation and served as a source for protein purification. The proteins (SdCen, N-SdCen, and C-SdCen) were purified as previously described for HsCen2 (*27*). The protein concentration was determined by spectrophotometry using extinction coefficients (ε) of 1490 and 2860 $M^{-1}\,cm^{-1}$ at 280 and 259 nm, respectively, based on the Tyr and Phe content.

Metal Removal and Cation Binding. SdCen was precipitated with 3% trichloroacetic acid and passed through a 40 cm × 1 cm Sephadex G-25 column equilibrated in 50 mM Tris-HCl (pH 7.5) and 150 mM KCl (buffer A). Typically, the contamination represents less than 2% of the total binding capacity. Total Ca^{2+} and Mg^{2+} concentrations were determined with a Perkin-Elmer 2380 atomic absorption spectrophotometer. Flow dialyses on 50 μM SdCen were conducted in the absence or presence of 2 mM Mg^{2+} at 25 °C in buffer A according to the modified method of Colowick and Womack (*35*). Treatment of the raw data and evaluation of the binding parameters was conducted as previously described (*36*). The data were analyzed using the Adair equation for three binding sites (for details, see ref *30*). In the flow dialysis experiment on a 2:1 mixture of ME and SdCen, 2 μM ME was present in the perfusion buffer (*27*). The antagonism between Ca^{2+} and Mg^{2+} was tested with the competition equation for each site: $K'_{Ca}/K'_{Ca.app} = 1 + K'_{Mg.comp}[Mg^{2+}]$, where K'_{Ca} and $K'_{Ca.app}$ are the intrinsic Ca^{2+} binding constants for a given site in the absence and presence of Mg^{2+}, respectively, and $K'_{Mg.comp}$ is the calculated Mg^{2+} binding constant for this site.

Interaction with Hydrophobic Probes. The Ca^{2+}-dependent changes in the hydrophobic patches of SdCen were followed by monitoring the fluorescence properties of 2-*p*-toluidinylnaphthalene 6-sulfonate (TNS) as described previously (*37*), using a Perkin-Elmer LS 50B spectrofluorometer. The Ca^{2+} dependence of the probe fluorescence enhancement was monitored starting with a solution in buffer A of 4 μM protein, 40 μM TNS, and 2 μM contaminating Ca^{2+} (measured by atomic absorption photometry); this solution was titrated with increasing Ca^{2+} or EGTA concentrations. The amount of free Ca^{2+} was calculated with WEBMAXC STANDARD. Mg^{2+} titrations were conducted on 10 μM metal-free protein in buffer A containing 1 mM EGTA.

Isothermal Titration Calorimetry. Calcium was removed from all buffers [50 mM MOPS and 100 or 500 mM NaCl (pH 7.4)] when they were passed through a Chelex 100 column (*31*). Centrins (SdCen, N-SdCen, and C-SdCen) in buffer [50 mM MOPS, 100 mM NaCl, and 50 mM EDTA (pH 7.4)] were stripped with buffer [50 mM MOPS and 500 mM NaCl (pH 7.4)] and desalted through a G25 column equilibrated in buffer [50 mM MOPS and 100 mM NaCl (pH 7.4)]. Thermodynamic parameters of molecular interactions between centrin and metal ions or target peptides were investigated by ITC using a VP-ITC instrument (MicroCal Inc., Northampton, MA). The protein, the metal ions, and the peptides were equilibrated in the same buffer containing 50 mM MOPS (pH 7.4), 100 mM NaCl, and $CaCl_2$ (1 mM), or EDTA (2 mM). Centrin at 15−45 μM in the calorimeter cell was titrated with the metal ions (0.5−1.0 mM) or the peptides (150−200 μM) by automatic injections of 5−10 μL. The first injection of 2 μL was ignored in the final data analysis. Integration of the peaks corresponding to each injection and correction for the baseline were accomplished using Origin-based software provided by the manufacturer. The fit of the data to an interaction model results in the stoichiometry, equilibrium binding constant (K_a), and enthalpy (ΔH) of complex formation. All the experiments were repeated twice and gave similar results. Control experiments, consisting of the injection of peptide solutions into the buffer, were performed to evaluate the heat of dilution.

Fluorimetric Titrations. Trp fluorimetry was used for monitoring the titration of centrin into the peptide solution. The experiments were performed on a Jasco FP777 spectrofluorometer (Jasco, Tokyo, Japan) equipped with a temperature control device. The fluorescence excitation wavelength was 295 nm, and fluorescence emission spectra were recorded between 290 and 410 nm at 25 °C, using quartz cuvettes. Samples were prepared in buffer A and studied at 25 °C. Formation of the complex was followed by changes in the microenvironment of the peptide Trp upon centrin titration, which in turn is reflected in fluorescence emission changes.

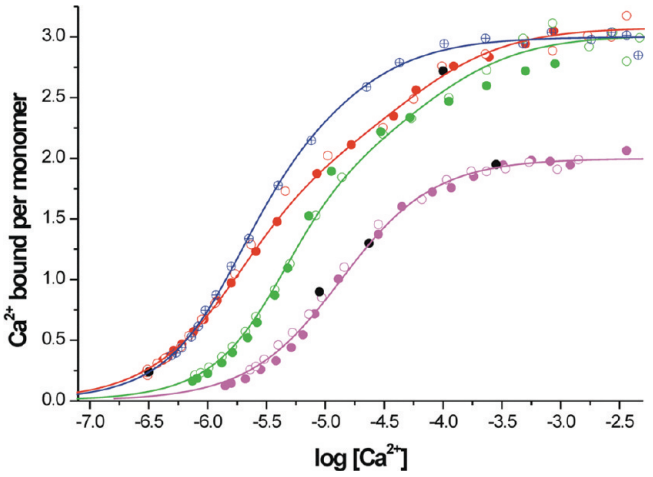

FIGURE 1: Ca^{2+} binding to SdCen measured by flow dialysis. Direct Ca^{2+} binding to recombinant SdCen was monitored by flow dialysis at 25 °C in 50 mM Tris-HCl (pH 7.5) and 150 mM KCl (buffer A). The protein concentration was 50 μM. Duplicate (empty and filled symbols) experiments are shown in the absence (red) or presence of 2 mM Mg^{2+} (green). The blue crossed symbols represent a flow dialysis on a 2:1 molar mixture of ME and SdCen. Results of similar duplicate experiments with N-SdCen in the absence of Mg^{2+} are colored magenta. The solid lines are the theoretical isotherms calculated with the Adair equation for three (SdCen) or two (N-SdCen) sites with the intrinsic constants listed in Table 1. The black circles represent results of equilibrium gel filtration experiments with SdCen and N-SdCen (no Mg^{2+}).

CD measurements were performed on a Jasco J-715 CD spectropolarimeter equipped with a Peltier temperature control device. Far-UV spectra were recorded between 200 and 250 nm at 22 °C using 1 mm quartz cells. Spectra were collected as an average of four scans, with a scan speed of 20 nm/min and a response time of 2 s. Samples were prepared in 10 mM Tris buffer (pH 7.5) and 20 mM NaCl. Thermal denaturation was followed by recording the ellipicity at 222 nm between 5 and 90 °C with a rate of temperature increase of 1 °C/min. The reversibility of the thermal unfolding process was assessed to be higher than 95%, by comparing the CD spectra at the beginning and at the end of the thermal cycle.

RESULTS

Ca^{2+} Binding Properties. (*i*) *Flow Dialysis Studies and Effect of Mg^{2+} and Melittin*. Flow dialysis on the apoprotein in the absence of Mg^{2+} yielded a biphasic isotherm (Figure 1), which leveled out at three bound Ca^{2+} ions per monomer. This stoichiometry suggests that under the experimental conditions SdCen has two high-affinity sites ($K_a \sim 3 \times 10^5$ M^{-1}, no cooperativity) and one moderate-affinity site ($K_a = 5.1 \times 10^4$ M^{-1}) (see Table 1a). In the presence of 2 mM Mg^{2+}, the Ca^{2+} binding isotherm of the two high-affinity sites is slightly shifted to the right, and according to the Adair analysis, only the affinity of one site is significantly decreased (4-fold). The flow dialysis was also performed on a 1:2 mixture of apo SdCen and ME, a model peptide that interacts with centrins (*27*, *30*). The isotherm shows

Table 1

(a) Intrinsic Ca^{2+} Binding Constants of SdCen in the Presence and Absence of 2 mM Mg^{2+} or Melittin Derived from the Stoichiometric Constants, Which Were Obtained after All the Data Had Been Fit to the Adair Equation for Three Sites

	putative EF-hands I and II		putative EF-hands III and IV	
	K'_1 (M^{-1})	K'_2 (M^{-1})	K'_3 (M^{-1})	K'_3 (M^{-1})
SdCen	3.0×10^5	3.4×10^5		5.1×10^4
SdCen with 2 mM Mg^{2+}	7.5×10^4	2.4×10^5		3.9×10^4
SdCen with 50 μM melittin	2.3×10^5	5.8×10^5		2.5×10^5
N-SdCen	6.0×10^4	8.0×10^4		

(b) Ca^{2+} Binding Constants of SdCen Determined Using the ITC Method

protein	K_1 (M^{-1})	ΔH_1 (kcal/mol)	K_2 (M^{-1})	ΔH_2 (kcal/mol)	K_3 (M^{-1})	ΔH_3 (kcal/mol)
SdCen	2.6×10^5	16.9	1.1×10^5	1.3	4.3×10^5	−7.9
N-SdCen	0.8×10^5	0.6	1.9×10^5	1.7		
C-SdCen	1.1×10^5	−18.7				

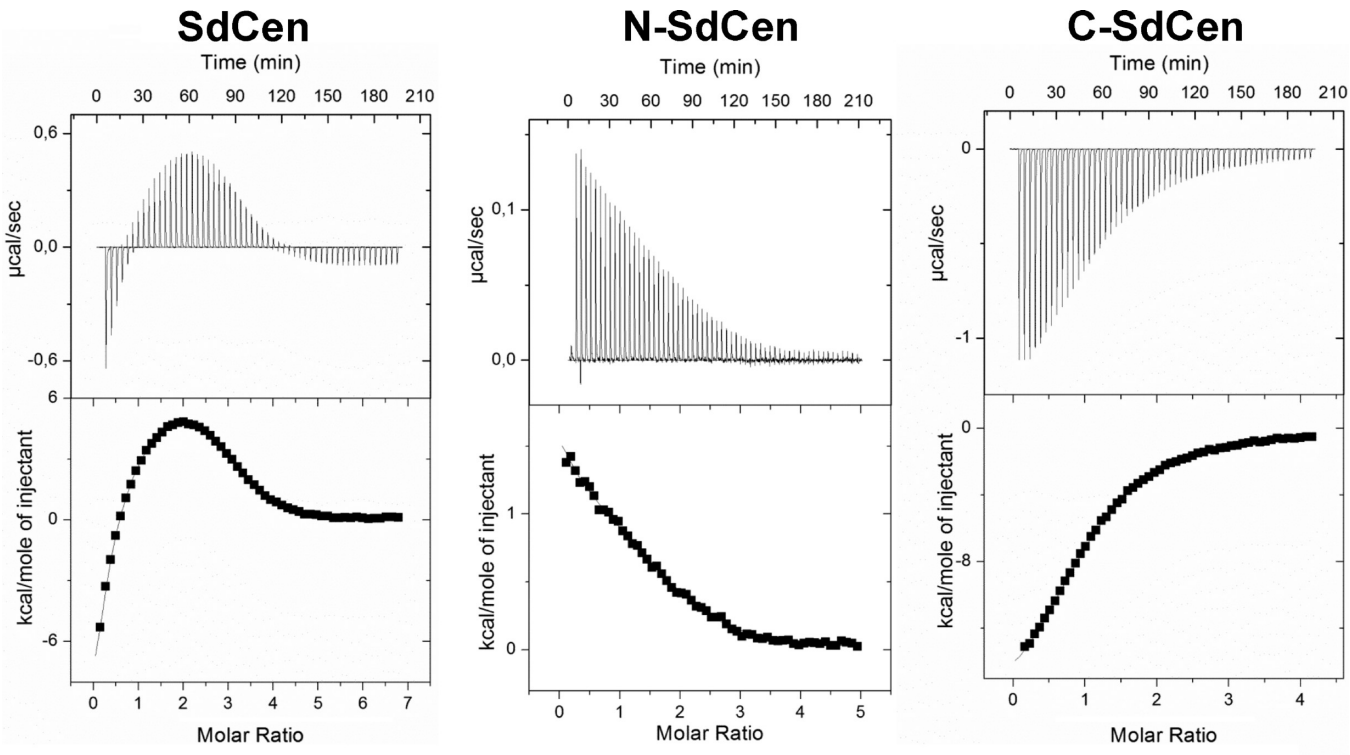

FIGURE 2: Ca^{2+} binding observed by isothermal titration calorimetry. Thermograms (top panels) and isotherms (bottom panels) of the titration of Ca^{2+} (0.5 mM) into 45 μM SdCen (left), 25 μM N-SdCen (middle), and 25 μM C-SdCen (right) at 30 °C.

the same stoichiometry, but a slightly higher affinity, especially for the single moderate-affinity site (4.9-fold increase in K'_3).

Recombinant N-SdCen binds two Ca^{2+} ions with a rather high mean affinity ($K_a = 7.5 \times 10^4$ M^{-1}) and a slight positive cooperativity ($n_H = 1.09$). Thus, the two high-affinity sites on whole SdCen reside in the N-terminal half, although in isolated N-SdCen this affinity is weakened by a factor of 4−5. This suggests that, contrary to the case of CaM and CrCen or other centrins, the presence of the C-terminal half enhances the Ca^{2+} affinity in the N-terminal half. The location of the high-affinity sites is corroborated by the fact that 2 mM Mg^{2+} shifts the binding curve of N-SdCen to the right to the same extent as in whole SdCen (not shown). As in CrCen (*31*) and in HsCen2 (*27*), the moderate-affinity Ca^{2+}-specific site is thus located in the C-terminal half of the SdCen, most probably site IV.

(*ii*) *Thermodynamics of Ca^{2+} Binding*. Isothermal titration calorimetry was used as an additional method to study the Ca^{2+} binding to the algal centrin. The solutions of SdCen, N-SdCen, and C-SdCen (25 μM) were titrated with a $CaCl_2$ solution (750 μM) in the same buffer as the protein [50 mM MOPS (pH 7.4) and 100 mM NaCl] at 30 °C. As shown in Figure 2, fitting the data for the SdCen integral protein with a three-site sequential binding model gives affinity values of 2.6×10^5, 1.1×10^5, and 4.3×10^5 M^{-1} (Table 1b). The titration of the isolated N-terminal domain (Figure 2) reveals two binding sites with positive enthalpy that should correspond to the endothermic binding sites observed in the integral protein. The fitting of the isotherm with a two-site sequential binding model gives binding constants of 0.8×10^5 and 1.9×10^5 M^{-1} (Table 1b), very similar to the value obtained by flow dialysis on isolated N-SdCen (Table 1a). The binding enthalpy

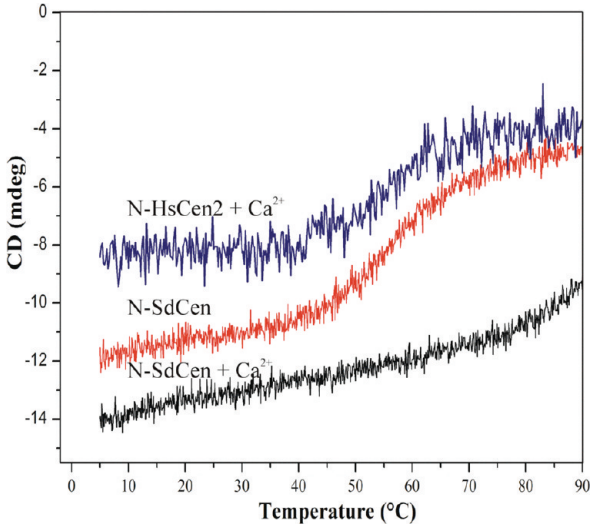

FIGURE 3: Thermal denaturation studied by CD. The CD denaturation curves of N-SdCen in the presence and the absence of Ca^{2+} and of N-HsCen2 in the presence of Ca^{2+} were recorded as the temperature dependence of the ellipticity at 222 nm. The rate of temperature increase was 1 °C/min.

is different from that of the endothermic binding site in the integral protein, suggesting that some differences may exist in the binding properties between the isolated domain and the integral protein, as also suggested by the dialysis experiments. An exothermic Ca^{2+} binding site ($K_a = 1.1 \times 10^5$ M^{-1}) has been detected in the isolated C-terminal domain, as indicated by the one-site fitting of the corresponding isotherm (Figure 2). Consequently, the exothermic binding site belongs to the C-terminal domain in the integral SdCen.

Ca^{2+}-Induced Conformational Changes. (*i*) *Secondary Structure and Structural Stability*. Ca^{2+} binding to SdCen induces a slightly more negative ellipticity in the far-UV CD spectrum (data not shown) as commonly observed for various centrins (*27*, *30*, *39*). This may be interpreted as a stabilization of some helical segments and/or a rearrangement of the helical elements within the tertiary structure (*40*). When Ca^{2+} binds, isolated N-SdCen also exhibits a significant decrease (more negative by ~10%) in ellipticity at 222 nm, suggesting a Ca^{2+}-dependent increase in α-helical content (*41*). More significantly, addition of Ca^{2+} increases considerably the thermal stability of the N-terminal domain, in contrast with the behavior of the N-terminal domain of HsCen2 (Figure 3). The metal-free form of N-SdCen displays a CD melting curve with a cooperative thermal transition at ~55 °C, similar to that of N-HsCen2 (*29*). The binding of Ca^{2+} to EF-hands I and II considerably increases the thermal stability of N-SdCen, which in the holo form shows a cooperative transition with a midtransition temperature above 90 °C (Figure 3). This is in contrast with the thermal denaturation of N-HsCen2 which has been shown to be insensitive to calcium ions (*29*).

(*ii*) *Tertiary Changes*. Metal-free SdCen enhances the fluorescence of the hydrophobic probe TNS 2-fold, with a maximum at 423 nm (Figure 4A). When Ca^{2+} binds, the fluorescence emission further increases (more than 8-fold) and is red-shifted to 432 nm. The large Ca^{2+}-induced fluorescence enhancement of TNS occurs in two steps: the major increase (66% of total enhancement) occurs at the very low $[Ca^{2+}]_{0.5}$ of 7 nM and is strongly cooperative, while the minor increase (34%) occurs at a $[Ca^{2+}]_{0.5}$ of 5 μM (Figure 4B). It can thus be inferred that two distinct hydrophobic surfaces are exposed with different Ca^{2+} sensitivities. Binding of

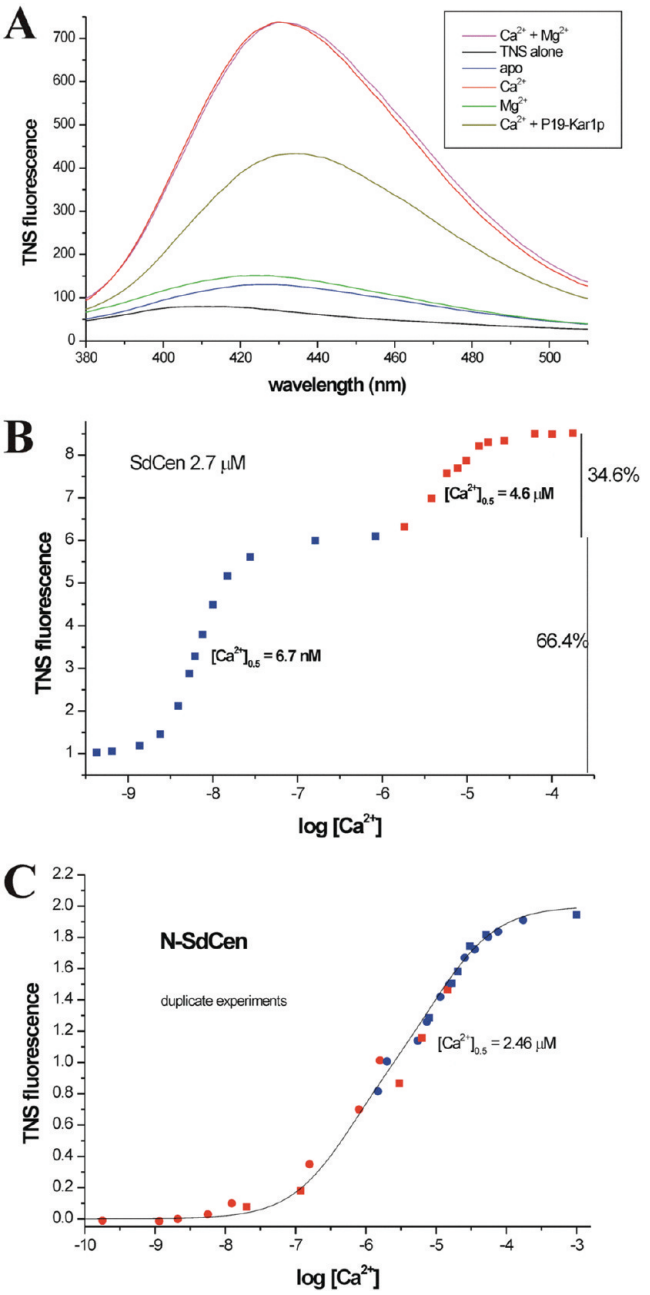

FIGURE 4: Ca^{2+}-dependent exposure of hydrophobic side chains. (A) Hydrophobic exposure was monitored, at 25 °C in 50 mM Tris-HCl (pH 7.5) and 150 mM KCl, with the hydrophobic probe TNS. Emission fluorescence spectra of TNS alone (black) and with 3 μM SdCen in the presence of 50 μM EGTA (blue), 1 mM Mg^{2+} (green), 1 mM Ca^{2+} (red), 1 mM Ca^{2+} and 1 mM Mg^{2+} (magenta), or 1 mM Ca^{2+} and 4 μM P19-Kar1 (yellow). (B) Dependence of the signal on the free Ca^{2+} concentration. The solution containing TNS and SdCen contained 2 μM contaminating Ca^{2+} and was titrated with EGTA (blue marks) or Ca^{2+} (red marks). For the EGTA titration, the amount of free Ca^{2+} was calculated as indicated in Materials and Methods. (C) Ca^{2+} dependence for N-SdCen. Same symbols as for panel B.

Mg^{2+} to the apoprotein leads to a slight but significant 16% increase (compare green and blue lines in Figure 4A) in fluorescence, without a red shift. This transition could be titrated and yielded a $[Mg^{2+}]_{0.5}$ of ~1 mM (data not shown), which is comparable to the small antagonistic effect in the flow dialysis experiments.

Metal-free N-SdCen enhances the fluorescence 3-fold. When Ca^{2+} binds, the TNS fluorescence further increases more than

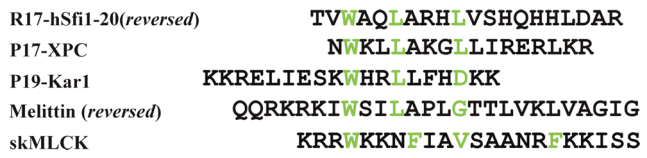

FIGURE 5: Sequences of the target peptides used in our experiments. The hydrophobic triad representing the centrin binding motif is colored green. Note that the sequences of R17-hSfi1 and melittin are reversed. skMLCK represents the CaM binding site of the skeletal muscle myosin light kinase with the anchoring residues in relative positions 1, 5, 8, and 14 (green).

7-fold and is red-shifted to 443 nm (data not shown). Interestingly, for the TNS−N-SdCen complex, the $[Ca^{2+}]_{0.5}$ value is 2.5 μM (Figure 4C), suggesting that the highly Ca^{2+}-sensitive step in the whole protein may be assigned to the N-terminal EF-hands. Again, the Ca^{2+} affinity is partially lost in isolated N-SdCen because the C-terminal part of the protein is removed.

Binding of Natural Target Peptides. As a regulatory protein, centrin should perform its cellular functions by interacting with other proteins. The specific target proteins of algal centrins are actually not known, but it is highly probable that the centrin targets in various organisms share a common binding motif. We therefore performed ITC measurements on the interaction between SdCen or its N-terminal and C-terminal domains with three natural target peptides, one derived from the DNA repair (nucleotide excision repair) human protein XPC (P17-XPC), another derived from the human centrosomal Sfi1 protein (R17-hSfi1), and the third derived from the yeast Kar1 protein (P19-Kar1) (Figure 5). The raw ITC data and the binding isotherms corresponding to the interaction of the first two peptides with SdCen in the presence or absence of Ca^{2+} are shown in Figure 6A, while the complete thermodynamic data for the three peptides are presented in Table 2. In the presence of Ca^{2+}, the binding isotherm could be fitted to only a two-site binding model, clearly indicating that the *S. dubia* centrin possesses two active binding sites for these peptides, in contrast to previously studied centrins in which only the C-terminal domain binds one target peptide (*30*, *42*, *43*). The binding affinity is different for the three peptides and for the two binding sites (Table 2).

The P17-XPC peptide binding to the N- and C-terminal fragments was also monitored by ITC. Under the experimental conditions (in the presence of Ca^{2+}), the isotherm for C-SdCen shows a single binding event with a stoichiometry of 1:1, and an association constant of 65.8×10^6 M^{-1}. The metal-free form of C-SdCen interacts with this peptide with a similar affinity (60.2×10^6 M^{-1}). The association constant for the isolated C-SdCen is 6.5-fold smaller than that of the high-affinity site in the integral protein in the presence of Ca^{2+}. These results confirm the capacity of the C-terminal domain of centrins to bind targets even in the absence of calcium (Figure 6B). In the presence of Ca^{2+}, N-SdCen exhibits a single binding site with affinity values depending on the target type (Figure 6B). The binding constants of isolated N-SdCen are larger than that of the same domain in the integral protein (19- and 3-fold higher for P17-XPC and R17-hSfi1, respectively). A plausible explanation is that the binding of a first molecule to the C-terminal domain (the high-affinity site) of the integral protein affects the binding of the second molecule to the N-terminal domain, probably through a steric effect.

In the absence of Ca^{2+}, the binding isotherms of SdCen show a simple single-site interaction (Figure 6A), indicating that one of the binding sites is inactive. The measured affinities for P17-XPC and R17-hSfi1 are 23- and 43-fold lower than that of the high-affinity site in the presence of Ca^{2+}. In contrast, apo N-SdCen does not display measurable peptide binding (Figure 6B), indicating again that the unique binding site in apo SdCen is situated in the C-terminal half. These observations demonstrate that the high- and low-affinity sites in holo SdCen correspond to the C-terminal and N-terminal domains, respectively.[2] Overall, the ITC results show that SdCen possesses two target binding sites, only one of which (in the N-terminal domain) is strictly dependent on Ca^{2+}.

The centrin binding motif was shown to consist of a hydrophobic triad ($W^1L^4L^8$) (Figure 5) that is deeply embedded in the hydrophobic cavity exposed by the C-terminal domain of centrins like HsCen2 (*44*) or yeast Cdc31 (*43*). The peptide derived from the Kar1 protein is somewhat different because it does not contain the third hydrophobic anchor residue (Figure 5), but we tested it to compare the characteristics of binding to the two algal centrins (SdCen and CrCen) (*45*). The profile for binding of P19-Kar1 to SdCen or N-SdCen is similar to the profile of binding of the two previous peptides (Table 2). The affinity for N-SdCen is very low in this case ($K_a = 3 \times 10^4$ M^{-1}), and this may explain why the binding to N-CrCen was not previously detected (*45*). The increase in the affinity of the isolated N-SdCen terminal domain is only marginal relative to that of the domain in the integral protein.

With its two active EF-hand domains, SdCen may present target binding modes similar to those shown by CaM. We were keen to ascertain the capacity of SdCen to bind a well-characterized CaM target peptide derived from the skeletal muscle myosin light chain kinase, exhibiting the 1-5-8-14 anchoring motif (Figure 5) (*46*). ITC titration of Ca^{2+}-bound SdCen by skMLCK shows indeed a strong interaction ($\sim 10^7$ M^{-1}) and a 1:1 stoichiometry (Figure 6C). In the absence of Ca^{2+}, the affinity decreases by a factor of 50, and the free energy components are very similar to those of the interaction of SdCen with centrin-specific peptides. The comparison of the interaction of integral SdCen and its halves with skMLCK in the presence of Ca^{2+} revealed that N-SdCen (Figure 6D) and C-SdCen (Figure 6D) display 100−150-fold lower affinities than intact SdCen, indicating that the high affinity is due to a wrapping up of the two halves around this peptide. This type of interaction of 1-5-8-14 type peptides is reminiscent of their interaction with CaM.

Fluorescence spectroscopy was also used to explore the target binding to SdCen or N-SdCen. These experiments are made possible by the presence of a Trp residue in each of the studied peptides, but not in SdCen. The fluorescence titration provided data about the binding strength and stoichiometry (see footnote 2), but also some structural information about the mode of binding. The emission fluorescence of the peptide Trp is very sensitive to formation of the complex, showing a significant blue shift and a 3−7-fold increase in intensity. This indicates that the indole group moved from an aqueous environment to an apolar cavity representing the binding pocket of each domain composed of paired EF-hands. Figure 7 illustrates the fluorescence spectra of P17-XPC and R17-hSfi1 in the presence of N-SdCen. Addition of

[2]The 2:1 complex of the Ca form of SdCen with P17-XPC and the 1:1 complex of the apo form of SdCen could be clearly shown by band shifts of SdCen in nondenaturating polyacrylamide electrophoreses when the peptide:SdCen ratios were increased from 0 to 2 (I. Durussel and J. A. Cox, data not shown). The same stoichiometries were observed when P17-XPC was titrated with the Ca and apo forms of SdCen, as monitored by the fluorescence of the peptide Trp (J. A. Cox, data not shown).

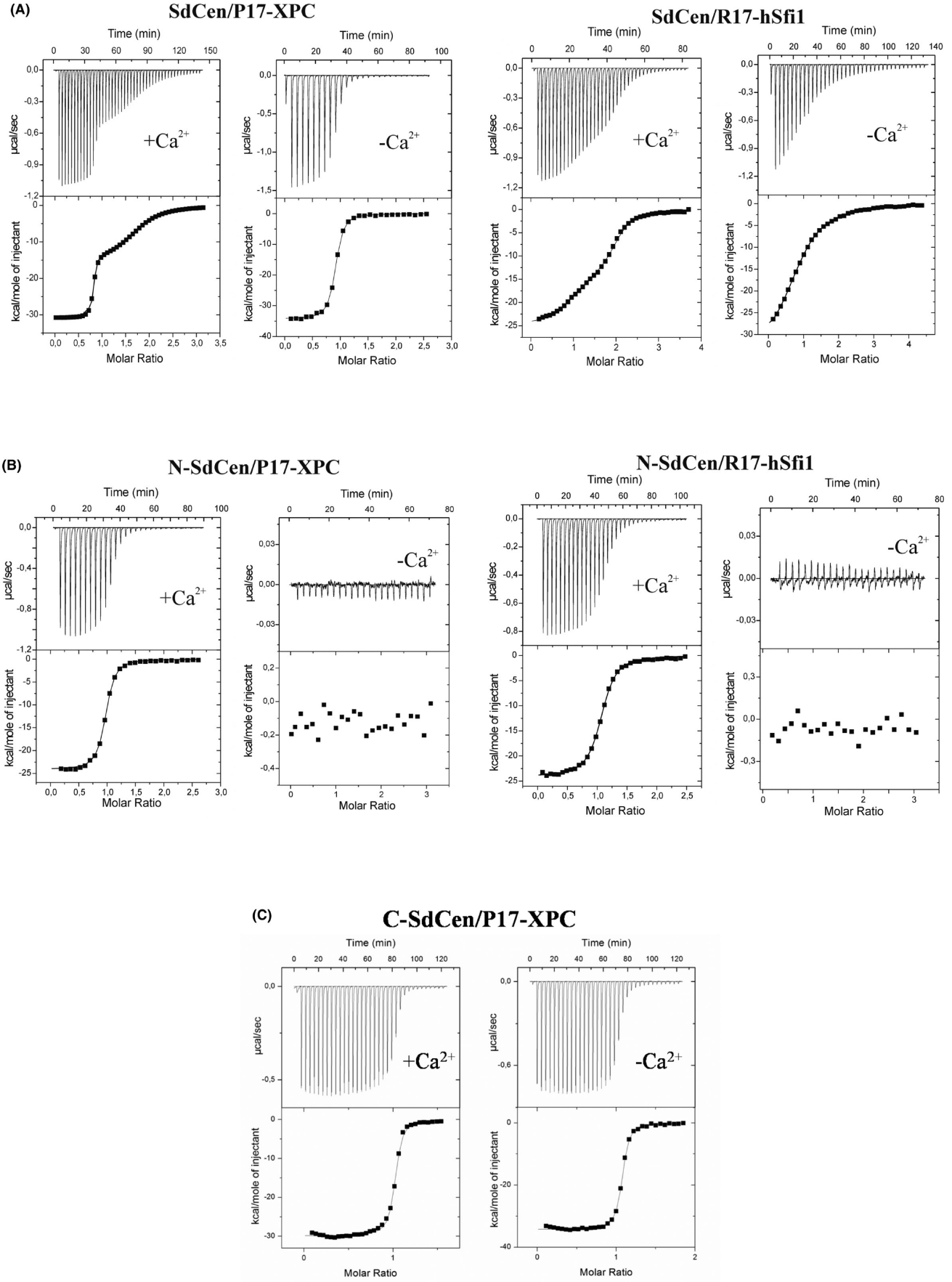

FIGURE 6. CONTINUED

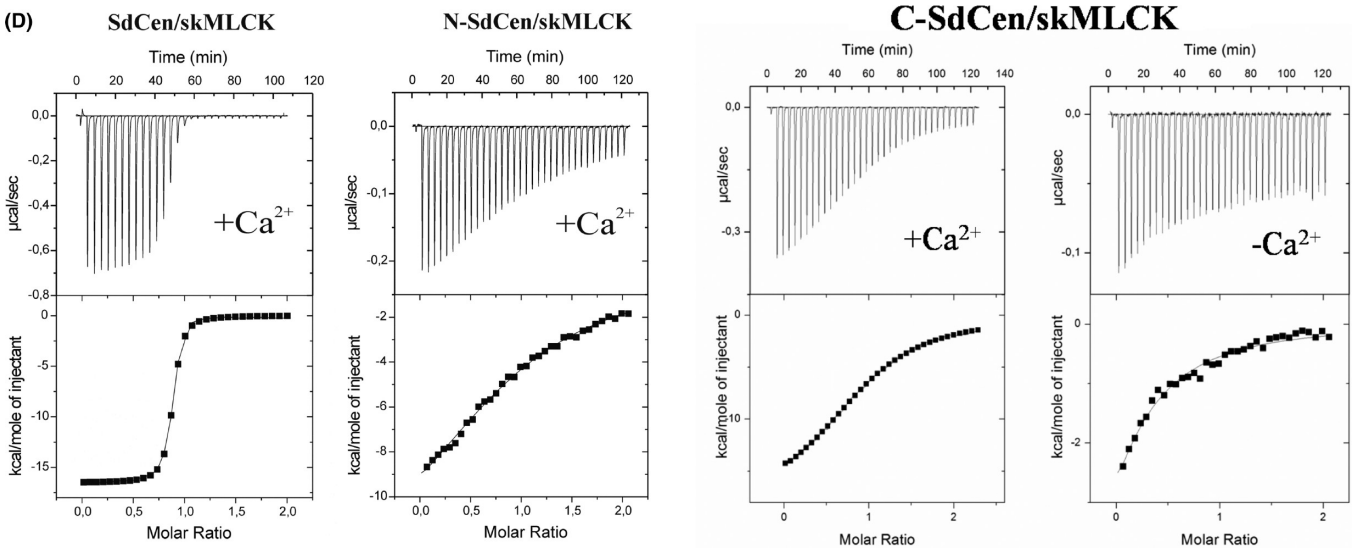

FIGURE 6: Peptide binding to SdCen (A), N-SdCen (B), and C-SdCen (C), studied by isothermal titration calorimetry. Thermograms (top panels) and binding isotherms (bottom panels) of the titration of P17-XPC, R17-hSfi1, or skMLCK (D) into SdCen or N-SdCen, in the presence and absence of Ca^{2+}, at 30 °C.

Table 2: Summary of the Thermodynamic Parameters of the Interaction between SdCen and Its N-Terminal and C-Terminal Domains with the Peptides Derived from Centrin Target Proteins[a]

protein (10 μM)	ligand (150 μM)	[Ca^{2+}] (mM)	n	K_a ($\times 10^6$ M^{-1}) (error)	ΔH (kcal/mol) (error)	ΔG (kcal/mol)	$T\Delta S$ (kcal/mol)
SdCen	P17-XPC	1	2	K_1 = 426 (67)	−31.3 (0.1)	−12.0	−19.3
				K_2 = 0.75 (0.07)	−16.9 (0.5)	−8.2	−8.7
		0	1	K = 19 (0.9)	−34.3 (0.1)	−10.1	−24.2
N-SdCen		1	1	K = 14 (1)	−24.1 (0.2)	−9.9	−14.2
		0	–	NB[c]	–	–	–
C-SdCen		1	1	K = 65.8 (5.3)	−29.8 (0.1)	−10.9	−18.9
		0	1	K = 60.2 (3.5)	−34.2 (0.09)	−10.8	−23.4
SdCen	R17-HsSfi1[b]	1	2	K_1 = 20 (4)	−25.6 (0.5)	−10.1	−15.5
				K_2 = 2.5 (0.2)	−12.1 (0.5)	−8.9	−3.2
		0	1	K = 0.49 (0.01)	−34.3 (0.3)	−7.8	−26.5
N-SdCen	R17-HsSfi1	1	1	K = 6.9 (0.3)	−24.1 (0.9)	−9.5	−14.6
		0	–	NB[c]	–	–	–
SdCen	P19-Kar1	1	2	K_1 = 39 (11)	−18.74 (0.04)	−10.5	−8.24
				K_2 = 0.03 (0.01)	−10 (1)	−6.2	−3.8
		0	1	K = 0.40 (0.01)	−29.7 (0.5)	−7.8	−21.9
N-SdCen		1	1	K = 0.043 (0.002)	−11.6 (0.2)	−6.4	−5.2
		0	–	NB[c]	–	–	–
SdCen	skMLCK	1	1	K = 18.3 (0.1)	−14.5 (0.54)	−10.1	−4.4
		0	1	K = 0.4 (0.03)	−28.8 (0.3)	−7.8	−21.0
N-SdCen		1	1	K = 0.15(0.03)	−15.2 (0.6)	−7.2	−8.0
		0	–	NB[c]	–	–	–
C-SdCen		1	1	K = 0.41(0.01)	−18.3 (0.3)	−7.8	−10.5
		0	1	K = 0.15(0.03)	−10.2 (0.5)	−7.2	−3.0
SdCen	mellitin	1	1	K = 32.7 (6)	4.23 (0.05)	10.4	6.15

[a]Samples are in MOPS buffer (pH 7.4) and 100 mM NaCl, in the presence (1 mM) and absence (2 mM EDTA) of Ca^{2+} ions. Experiments were conducted at 30 °C. [b]The ligand concentration was 200 μM in this experiment. [c]No binding observed under these experimental conditions.

N-SdCen to P17-XPC leads to a 3-fold increase in Trp fluorescence, accompanied by a blue shift from 352 to 321 nm (isosbestic point at 365 nm) (Figure 7A). The apo form does not notably change the fluorescence properties of the peptide Trp, in agreement with the ITC data. Addition of an excess of 2.3 mM EGTA to the complex formed in the presence of 1.5 mM Ca^{2+} does not dissociate the complex, suggesting a strong increase in Ca^{2+} affinity. The R17-hSfi1 peptide displays the same conformational changes when interacting with N-SdCen, except that the fluorescence increase is smaller and less blue-shifted (from 355 to 321 nm, isosbestic point at 358 nm) (Figure 7B). Fluorescence titration of the yeast Sfi1 repeat by the N-terminal domain of CrCen also induces a blue shift in λ_{max} from 355 to 335 nm, but in contrast with the N-SdCen case, a substantial quenching of the fluorescence is observed (*48*). The available data do not allow an explanation of this difference in the titration behavior of the two algal centrins.

DISCUSSION

Calcium and the Cell Cycle. The precise role of Ca^{2+} in the cell cycle is hotly debated. Cell cycle transients were observed in many cell types, including echinoderms (*49*), see urchin embryos (*50*),

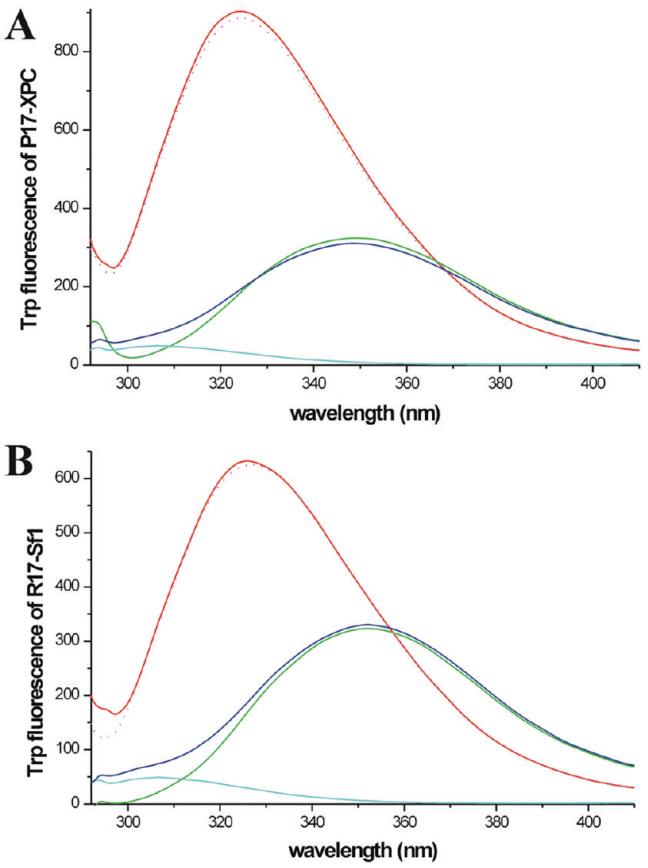

FIGURE 7: Binding of N-SdCen to P17-XPC and to R17-hSfi1, measured by Trp fluorescence. P17-XPC (3.2 μM) (A) or R17-Sfi1 (B) was titrated by N-SdCen: green for the peptide alone, cyan for 4 μM N-SdCen alone, solid red for the peptide with 4 μM N-SdCen in the presence of 1.5 mM Ca^{2+}, dashed red for the peptide after neutralization of Ca^{2+} by an excess of 2.5 mM EGTA, and blue for the peptide with 4 μM N-SdCen in the presence of 1 mM EGTA.

and mammalian cells in culture (*51*), but no such transients were detected in dividing mouse embryos (*52*). Since also in vertebrates, blocking of the Ca^{2+} signal prevents mitosis, Whitaker (*53*) hypothesized that the changing endoplasmic reticulum architecture creates microdomains of Ca^{2+} (not visible by whole cell Ca^{2+} imaging) around the mitotic spindles and the centrosomes. Centrosome duplication and segregation in the prophase are also related to Ca^{2+} signals (*54*). It is well-documented that CaM, via CaMKII and calcineurin, is an important relay protein of the Ca^{2+} signal, but an important role for centrins in Ca^{2+}-mediated centrosome duplication must also be envisioned (*55*). The discovery of Sfi1 (*13*) led Salisbury to postulate a novel mechanism of cell duplication (*55*) based on a "unit of duplication", a γ-tubulin nucleating complex associated with a centrin/Sfi1 fiber via the N-terminus of Sfi1. Centriole (SPB) duplication requires either C-terminal tail-to-tail homodimerization of Sfi1, thus forming the SPB in yeast, or oligomerization (a 9-mer, forming the cartwheel) in green algae (*56*) and likely in vertebrates (where a well-structured precursor cartwheel is less often seen). The centrin−Sfi1 complexes should also play an important role in the structure and function of the Ca^{2+}-sensitive fibers connecting the centrioles among them or with other cellular structures.

Calcium Binding Capacity of Centrins. Generally, the CaM superfamily members have four functional Ca^{2+} binding sites, one pair in each domain of the protein. Usually, these sites are quite specific for Ca^{2+}, i.e., interact poorly or do not interact with Mg^{2+}, and have a moderate affinity for Ca^{2+} under physiological conditions. The centrins also belong to the CaM superfamily but display a greater variance in their divalent cation binding properties, at least in their N-terminal domain. *C. reinhardtii* centrin kept three functional EF-hands with two high-affinity sites in the N-terminal domain and one site of moderate affinity (K_a = $2-4\times10^4$ M^{-1} for EF-hand IV) in the C-terminal domain (*31*, *45*). HsCen2 binds only one Ca^{2+} per monomer with a high affinity ($K_a \sim 10^5$ M^{-1}) and strict Ca^{2+} specificity (*27*). HsCen3 shows still another binding profile with one high-affinity Ca^{2+}/Mg^{2+}-mixed site in the N-terminal domain and two low-affinity ($K_a \sim 7\times10^3$ M^{-1}) Ca^{2+}-specific sites in the C-terminal domain (*30*). In this study, we showed that SdCen possesses three sites, two in the N-terminal domain and one site in the C-terminal domain, like CrCen. The Mg^{2+} affinity cannot be probed by direct methods, but a weak Ca^{2+}/Mg^{2+} antagonism at one site is clear from our binding data.

The N-terminal domain (without the variable 20-residue N-terminal segment) of SdCen is 95% identical in sequence with CrCen, while the C-terminal domain is 78% identical in sequence with CrCen (Figure S1 of the Supporting Information). This comparison and our experimental data suggest that, as in CrCen (*45*) and other centrins (HsCen2), EF-hand III has a very low affinity. The moderate affinity is associated with EF-hand IV, and the two high-affinity sites are EF-hand I and EF-hand II, as in CrCen. TNS data suggest that the K_d for Mg^{2+} is around 1 mM. Again, this points to similarity between SdCen and CrCen, for which a $K_{d.comp}$ of 2 mM can be calculated from the data in ref *57*. Our binding data for N-SdCen confirm our assignation of EF-hand I and EF-hand II as the high-affinity sites. However, in contrast with CrCen (*31*, *57*), the isolated N-SdCen has weakened Ca^{2+} binding affinity relative to that of the whole protein. It is intriguing that the structural independence of the two EF-hand domains, well-documented for CrCen (*31*), HsCen2 (*28*, *29*), and CaM (*58*), is much less the rule for SdCen: this study shows that the N-terminal Ca^{2+} affinity, the hydrophobic profile, and the interaction with peptides are significantly different in the integral protein versus the isolated domain.

The strong TNS fluorescence enhancement by the Ca^{2+}-loaded form clearly is reminiscent of the one that occurs in CaM and in other centrins and corresponds to the exposure of one or two hydrophobic patches on the surface of the protein. The Ca^{2+} dependence of hydrophobic exposure is clearly biphasic with one transition in the nanomolar range and one in the micromolar Ca^{2+} range. In CrCen, too, there are two hydrophobic patches: one in the N-terminal domain and one in the C-terminal domain (*48*). In HsCen2 (*27*) and HsCen3 (*30*), there is no hydrophobic patch associated with the N-terminal domain, and the changes observed in the C-terminal domain occur at a relatively high Ca^{2+} concentration, as expected for the moderate Ca^{2+} affinity in the C-terminal domain. These hydrophobic patches are important for SdCen activity since they are for a great part hidden in the complex of Ca^{2+}-loaded SdCen with P19-Kar1 (Figure 4A).

Whereas the C-terminal domain of the centrins studied to date displays well-conserved Ca^{2+} binding properties, their N-terminal domains underwent profound modifications during evolution: HsCen2 [and HsCen1 (J. A. Cox, unpublished data)] lost the potential to bind Ca^{2+} in the N-terminal domain, whereas the N-terminal domain of HsCen3 still binds Ca^{2+}, leading to conformational changes, but serves only for the purpose of a transition from a molten globule state to a compact conformation,

without formation of a hydrophobic surface (*30*). However, the N-terminal domain of the green algal centrins exhibits two high-affinity sites for Ca^{2+} and forms a hydrophobic surface, and its subsequent interaction with target peptides is strictly dependent on Ca^{2+}.

Target Binding Properties. In agreement with the metal ion binding properties, SdCen exhibits specific target binding features, including the number of binding sites, the strength of binding, and the Ca^{2+} dependence. Here we focus on the thermodynamic parameters of the interaction of SdCen with three peptides derived from known centrin targets: XPC, hSfi1, and Kar1.

The Ca^{2+}-loaded form of SdCen possesses two distinct binding sites for each of the three peptides, with different affinities. The enthalpy change is the sole driving force for both binding steps. The thermodynamic characteristics of the high-affinity site are similar to those of HsCen2, which binds the peptide only in the C-terminus. The apo form of SdCen still binds 1 mol of peptide, but the affinity was more than 20−100-fold lower. We attributed this to the high-affinity site (the C-terminal domain) because N-SdCen binds one peptide with lower affinity, and this binding is strictly dependent on Ca^{2+}. The strongest binding to the high-affinity site is exhibited by the P17-XPC peptide that possesses a "canonical" centrin binding motif, the hydrophobic triad $W^1L^4L^8$ (*44*). The R17-hSfi1 peptide also possesses this motif provided that its sequence is "read" in a reverse direction (*14*) (Figure 5). The two peptide helices in the complex with centrin are oriented in a reverse direction so that the negative pole of the R17-hSfi1 dipole interacts in an unfavorable way with side chain negative charges of the centrin G-helix (*59*). This may explain the 20-fold reduction in the C-terminal domain affinity for R17-hSfi1 relative to the P17-XPC peptide. In contrast, the second binding step of R17-hSfi1 is 3-fold faster than the corresponding one of P17-XPC. Thus, R17-hSfi1 has a stronger preference for the N-terminal domain of SdCen, emphasizing the significance of the N-terminal domain interactions with centrosomal proteins. The much lower affinity of P19-Kar1 should be related to the presence of an acidic side chain in place of the third hydrophobic residue (L^8) of the triad (Figure 5).

The Ca^{2+}-dependent binding to SdCen and N-SdCen markedly changes the Trp fluorescence of peptides P17-XPC, R17-hSfi1, and P19-Kar1, strongly suggesting that the indole group of the targets becomes deeply embedded in a hydrophobic pocket of SdCen, as in the case of HsCen2 (*41*), CrCen (*45*), or Cdc31 (*43*). This points to a critical role of the target Trp in the binding to various centrins, as it is also the case for target peptides of CaM.

The diversity of Ca^{2+} and target binding of centrins, judging from previous work and our data, are schematically illustrated in Figure 8A. Although belonging to the same phylogenic subfamily as human centrins 1 and 2, SdCen, and probably all the green algal centrins, conserved high-affinity Ca^{2+} binding sites in the N-terminal domain that control conformational opening and target binding. Sequence comparison of centrins of various origin shows that algal centrins have two common distinctive properties in the second calcium binding loop of the N-terminal domain: one is an acidic pair in X (Asp) and −X (Asp), and the second is the presence of a Glu residue in position 12 of the loop. Indeed, introduction of an X,−X acid pair (positions 1 and 9 in the loop) increased significantly the Ca^{2+} affinity through a reduction in the ion dissociation rate (*60*). Also, the longer chain of a Glu in position 12 is suited for an optimal bidentate coordination of the divalent cation (*61*). These two parameters may be determinants

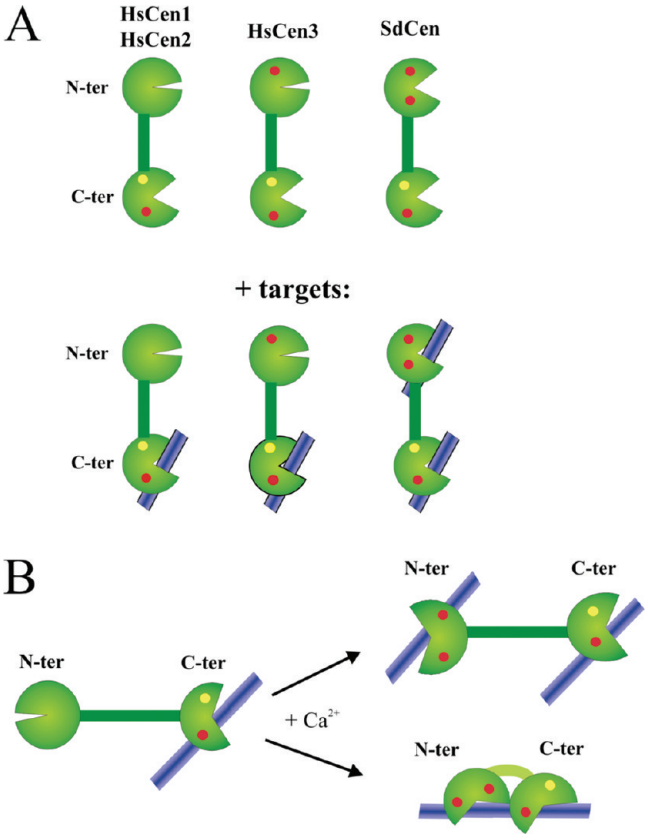

FIGURE 8: (A) Different modes of binding of centrins to calcium and target according to the available data. The N- and C-terminal domains are shown as two types of circle sectors representing closed and open conformations. The high and low affinities for calcium of the EF-hands are shown by red and yellow circles, respectively. Bound target peptides are shown as small blue bars. (B) Possible Ca^{2+}-controlled target binding modes specific for SdCen (and probably for all algal centrins).

for the unique properties of the N-terminal domain of algal centrins (Figure S1 of the Supporting Information). Interestingly, analysis of angiosperm centrin sequences shows that the two specific properties of the second EF-hand motif are also highly conserved in flowering plants, suggesting that their functional properties may be similar to those of algal centrins (Figure S2 of the Supporting Information).

Functional Implications. The contractile fibers linking the two centrioles may play an important functional role not only in anchoring the basal body (centrosome) to the perinuclear space but also in controlling the initiation of centriole duplication (*62*). By analogy with structural observations in yeast SPB (*43*), one can consider these fibers as mainly composed of Sfi1 and centrin proteins. The Ca^{2+} sensitivity of centrins in these array fibers could constitute the regulatory component for the Ca^{2+}-controlled centriole duplication or cell cycle progress.

Our study is part of a major project that aims to understand the mode of action and functional diversity of centrins. Sequence comparison and a number of functional properties, including Ca^{2+} binding affinities, Ca^{2+}/Mg^{2+} selectivity, and Ca^{2+} sensitivity of target binding, support the hypothesis that SdCen is very similar to CrCen. These green alga centrins resemble CaM, the most representative member of the CaM superfamily, in the sense that Ca^{2+}-regulated conformational changes allow hydrophobic exposure in both domains; however, the green alga centrins interact with two centrin-specific target molecules, whereas CaM

forms generally a 1:1 complex with its targets (*43*). This difference may come from the sequence of the target fragment rather than from the structural variation in the centrin domains. Indeed, our experiments with a CaM-specific target (skMLCK) showed that SdCen is able to bind a peptide possessing a hydrophobic anchoring residue in the 14th position from the Trp, forming a compact structure with the peptide wrapped up by the two halves of centrin (L. Radu et al., unpublished results).

Physiologically relevant complexes may require the binding of two molecules of the same target protein, one to each half, and the green alga centrins may act as linkers between two large molecules. Moreover, the Ca^{2+} sensitivity of the interaction of the N-terminal domain with target fragments suggests how the cellular function of SdCen (and probably of the other green algal centrins) is regulated by the Ca^{2+} signal (Figure 8B). While the C-terminal domain with its higher target affinity and lower Ca^{2+} sensitivity may be constitutively linked to one target, an increase in the local Ca^{2+} concentration triggers a secondary interaction with identical or distinct target molecules, resulting in structural and/or dynamics changes of local cellular assemblies. It is not actually known whether binding motifs resembling the skMLCK peptide may be encountered in natural centrin targets. Our results show that by its conformational flexibility and plasticity SdCen may bind various motifs in different interaction modes (Figure 8B).

ACKNOWLEDGMENT

We thank Jemila Houacine and Dora Grecu for enthusiastic participation in the preliminary and last experiments, respectively.

SUPPORTING INFORMATION AVAILABLE

Supplementary data. This material is available free of charge via the Internet at http://pubs.acs.org.

REFERENCES

1. Schiebel, E., and Bornens, M. (1995) In search of a function for centrins. *Trends Cell Biol. 5*, 197–201.
2. Salisbury, J. L. (1995) Centrin, centrosomes, and mitotic spindle poles. *Curr. Opin. Cell Biol. 7*, 39–45.
3. Salisbury, J. L., Baron, A., Surek, B., and Melkonian, M. (1984) Striated flagellar roots: Isolation and partial characterization of a calcium-modulated contractile organelle. *J. Cell Biol. 99*, 962–970.
4. Huang, B., Mengersen, A., and Lee, V. D. (1988) Molecular cloning of cDNA for caltractin, a basal body-associated Ca^{2+}-binding protein: Homology in its protein sequence with calmodulin and the yeast CDC31 gene product. *J. Cell Biol. 107*, 133–140.
5. Sanders, M. A., and Salisbury, J. L. (1994) Centrin plays an essential role in microtubule severing during flagellar excision in *Chlamydomonas reinhardtii*. *J. Cell Biol. 124*, 795–805.
6. Zhu, J.-K., Bressan, R., and Hasegawa, P. (1992) An *Atriplex nummularia* cDNA with sequence relatedness to the algal caltractin gene. *Plant Physiol. 99*, 1734–1735.
7. Baum, P., Furlong, C., and Byers, B. (1986) Yeast gene required for spindle pole body duplication: Homology of its product with Ca^{2+}-binding proteins. *Proc. Natl. Acad. Sci. U.S.A. 83*, 5512–5516.
8. Wolfrum, U. (1992) Cytosqueletal elements in arthropod sensilla and mammalian photoreceptors. *Biol. Cell 76*, 373–381.
9. Errabolu, R., Sanders, M. A., and Salisbury, J. L. (1994) Cloning of a cDNA encoding human centrin, an EF-hand protein of centrosomes and mitotic spindle poles. *J. Cell Sci. 107*, 9–16.
10. Lee, V. D., and Huang, B. (1993) Molecular cloning and centrosomal localization of human caltractin. *Proc. Natl. Acad. Sci. U.S.A. 90*, 11039–11043.
11. Wolfrum, U., Giesl, A., and Pulvermüller, A. (2002) Centrins, a novel group of Ca^{2+}-binding proteins in vertebrate photoreceptor cells. In Photoreceptors and Calcium (Baehr, W., and Palczewski, K., Eds.) pp 155−178, Kluwer Academic, New York.
12. Bornens, M., and Azimzadeh, J. (2007) Origin and evolution of the centrosome. *Adv. Exp. Med. Biol. 607*, 119–129.
13. Kilmartin, J. V. (2003) Sfi1p has conserved centrin-binding sites and a function in budding yeast spindle body duplication. *J. Cell Biol. 162*, 1211–1221.
14. Martinez-Sanz, J., Yang, A., Blouquit, Y., Duchambon, P., Assairi, L., and Craescu, C. T. (2006) Binding of human centrin 2 to the centrosomal protein hSfi1. *FEBS J. 273*, 4504–4515.
15. Salisbury, J. L. (2004) Centrosomes: Sfi1p and centrin unravel structural riddle. *Curr. Biol. 14*, R27–R29.
16. Salisbury, J. L., Suino, K. M., Busby, R., and Springett, M. (2002) Centrin-2 is required for centriole duplication in mammalian cells. *Curr. Biol. 12*, 1287–1292.
17. Marshall, W. F., Vucica, Y., and Rosenbaum, J. L. (2001) Kinetics and regulation of de novo centriole assembly. Implications for the mechanism of centriole duplication. *Curr. Biol. 11*, 308–317.
18. Paoletti, A., Bordes, N., Haddad, R., Schwartz, C. L., Chang, F., and Bornens, M. (2003) Fission yeast cdc31p is a component of the half-bridge and controls SPB duplication. *Mol. Biol. Cell 14*, 2793–2808.
19. Koblenz, B., Schoppmeier, J., Grunow, A., and Lechtreck, K.-F. (2003) Centrin deficiency in *Chlamydomonas* causes defects in basal body replication, segregation and maturation. *J. Cell Sci. 116*, 2635–2646.
20. Selvapandiyan, A., Debrabant, A., Duncan, R., Muller, J., Salotra, P., Sreenivas, G., Salisburry, J. L., and Nakhasi, H. L. (2004) Centrin gene disruption impairs stage-specific basal body duplication and cell cycle progression in *Leishmania*. *J. Biol. Chem. 279*, 25703–35710.
21. Araki, M., Masutani, C., Takemura, M., Uchida, A., Sugasawa, K., Kondoh, J., Ohkuma, Y., and Hanaoka, F. (2001) Centrosome protein centrin 2/caltractin 1 is part of the *xeroderma pigmentosum* group C complex that initiates global genome nucleotide excision repair. *J. Biol. Chem. 276*, 18665–18672.
22. Giessl, A., Pulvermuller, A., Trojan, P., Park, J. H., Choe, H.-W., Ernst, O. P., Hofmann, K. P., and Wolfrum, U. (2004) Differential expression and interaction with the visual G-protein transducin of centrin isoforms in mammalian photoreceptor cells. *J. Biol. Chem. 279*, 51472–51481.
23. Gonda, K., Yoshida, A., Oami, K., and Takahashi, M. (2004) Centrin is essential for the activity of the ciliary reversal-coupled voltage-gated Ca^{2+} channels. *Biochem. Biophys. Res. Commun. 323*, 891–897.
24. Guerra, C., Wada, Y., Leick, V., Bell, A., and Satir, P. (2003) Cloning, localization, and axonemal function of *Tetrahymena* centrin. *Mol. Biol. Cell 14*, 251–261.
25. Fischer, T., Rodriguez-Navarro, S., Pereira, G., Racz, A., Schiebel, E., and Hurt, E. (2004) Yeast centrin Cdc31 is linked to the nuclear mRNA export machinery. *Nat. Cell Biol. 6*, 840–848.
26. Resendes, K. K., Rasala, B. A., and Forbes, D. J. (2008) Centrin 2 localizes to the vertebrate nuclear pore and plays a role in mRNA and protein export. *Mol. Cell. Biol. 28*, 1755–1769.
27. Durussel, I., Blouquit, Y., Middendorp, S., Craescu, C. T., and Cox, J. A. (2000) Cation- and peptide-binding properties of human centrin 2. *FEBS Lett. 472*, 208–212.
28. Matei, E., Miron, S., Blouquit, Y., Duchambon, P., Durussel, I., Cox, J. A., and Craescu, C. T. (2003) The C-terminal half of human centrin 2 behaves like a regulatory EF-hand domain. *Biochemistry 42*, 1439–1450.
29. Yang, A., Miron, S., Duchambon, P., Assairi, L., Blouquit, Y., and Craescu, C. T. (2006) The N-terminal domain of human centrin 2 has a closed structure, binds calcium with a very low affinity, and plays a role in the self-assembly. *Biochemistry 45*, 880–889.
30. Cox, J. A., Durussel, I., Firanescu, C., Blouquit, Y., Duchambon, P., and Craescu, C. T. (2005) Calcium and magnesium binding to human centrin 3 and interaction with target peptides. *Biochemistry 44*, 840–850.
31. Veeraraghavan, S., Fagan, P. A., Hu, H., Lee, V., Harper, J. F., Bessie, H., and Chazin, W. J. (2002) Structural independence of the two EF-hand domains of caltractin. *J. Biol. Chem. 277*, 28564–28571.
32. Salisbury, J. L. (1998) Roots. *J. Eukaryotic Microbiol. 45*, 28–32.
33. Geimer, S., and Melkonian, M. (2004) The ultrastructure of the *Chlamydomonas reinhardtii* basal apparatus: Identification of an early marker of radial asymmetry inherent in the basal body. *J. Cell Sci. 117*, 2663–2674.
34. Maulet, Y., and Cox, J. A. (1983) Structural changes in melittin and calmodulin upon complex formation and their modulation by calcium. *Biochemistry 22*, 5680–5686.
35. Colowick, S. P., and Womack, F. C. (1969) Binding of diffusible molecules by macromolecules: Rapid measurement by rate of dialysis. *J. Biol. Chem. 244*, 774–747.
36. Cox, J. A. (1996) Guidbook to the Calcium-Binding Proteins (Celio, M. R., Pauls, T., and Schwaller, B., Eds.) Oxford University Press, Oxford, U.K.

37. Durussel, I., Méhul, B., Bernard, D., Schmidt, R., and Cox, J. A. (2002) Cation- and peptide-binding properties of human calmodulin-like skin protein. *Biochemistry 41*, 5439–5448.
38. Gifford, J. L., Walsh, M. P., and Vogel, H. J. (2007) Structures and metal-ion-binding properties of the Ca^{2+}-binding helix-loop-helix EF-hand motifs. *Biochem. J. 405*, 199–221.
39. Wiech, H., Geier, B. M., Paschke, T., Spang, A., Grein, K., Steinkötter, J., Melkonian, M., and Schiebel, E. (1996) Characterization of green alga, yeast, and human centrins. Specific subdomain features determine functional diversity. *J. Biol. Chem. 271*, 22453–22461.
40. Gagné, S. M., Tsuda, S., Li, M. X., Chandra, M., Smillie, L. B., and Sykes, B. D. (1994) Quantification of the calcium-induced secondary structural changes in the regulatory domain of troponin-C. *Protein Sci. 3*, 1961–1974.
41. Yang, A., Miron, S., Mouawad, L., Duchambon, P., Blouquit, Y., and Craescu, C. T. (2006) Flexibility and plasticity of human centrin 2 binding to the protein XPC from nuclear excision repair. *Biochemistry 45*, 3653–3663.
42. Popescu, A., Miron, S., Blouquit, Y., Duchambon, P., and Craescu, C. T. (2003) Xeroderma pigmentosum group C protein possesses a high affinity binding site for human centrin 2 and calmodulin. *J. Biol. Chem. 278*, 40252–40261.
43. Li, S., Sandercock, A. M., Conduit, P., Robinson, C. V., Williams, R. L., and Kilmartin, J. V. (2006) Structural role of Sfi1p-centrin filaments in budding yeast spindle pole body duplication. *J. Cell Biol. 173*, 867–877.
44. Charbonnier, J.-B., Renaud, E., Miron, S., Le Du, M. H., Blouquit, Y., Duchambon, P., Christova, P., Shosheva, A., Rose, T., Angulo, J. F., and Craescu, C. T. (2007) Structural, thermodynamic and cellular characterization of human centrin 2 interaction with *xeroderma pigmentosum* group C protein. *J. Mol. Biol. 373*, 1032–1046.
45. Hu, H., Sheehan, J. H., and Chazin, W. J. (2004) The mode of action of centrin. Binding of Ca^{2+} and a peptide fragment of Kar1p to the C-terminal domain. *J. Biol. Chem. 279*, 50895–50903.
46. Rhoads, A. R., and Friedberg, F. (1997) Sequence motifs for calmodulin recognition. *FASEB J. 11*, 331–340.
47. Ikura, M., Clore, G. M., Gronenborn, A. M., Zhu, G., Klee, C. B., and Bax, A. (1992) Solution structure of a calmodulin-target peptide complex by multidimensional NMR. *Science 256*, 632–638.
48. Sheehan, J. H., Bunick, C. G., Hu, H., Fagan, P. A., Meyn, S. M., and Chazin, W. J. (2006) Structure of the N-terminal calcium sensor domain of centrin reveals the biochemical basis for domain-specific function. *J. Biol. Chem. 281*, 2876–2881.
49. Kahl, C. R., and Means, A. R. (2003) Regulation of cell cycle progression by calcium/calmodulin-dependent pathways. *Endocr. Rev. 24*, 719–736.
50. Poenie, M., Alderton, J., Tsien, R. Y., and Steinhardt, R. (1985) Changes of free calcium levels with stages of the cell division cycle. *Nature 315*, 147–149.
51. Ratan, R. R., Shelanski, M., and Maxfield, F. R. (1986) Transition from metaphase is accompanied by local changes in cytoplasmic free calcium in Pt K2 kidney epithelial cells. *Proc. Natl. Acad. Sci. U.S.A. 83*, 5136–5140.
52. Whitaker, M., and Larman, M. G. (2001) Calcium and mitosis. *Semin. Cell Dev. Biol. 12*, 53–58.
53. Whitaker, M. (2006) Calcium microdomains and cell cycle control. *Cell Calcium 40*, 585–592.
54. Matsumoto, Y., and Maller, J. L. (2002) Calcium, calmodulin, and CaMKII requirement for initiation of centrosome duplication in *Xenopus* egg extracts. *Science 295*, 499–502.
55. Salisbury, J. L. (2007) A mechanistic view on the evolutionary origin for centrin-based control of centriole duplication. *J. Cell. Physiol. 213*, 420–428.
56. Lechtreck, K. F., and Grunow, A. (1999) Evidence for a direct role of nascent basal bodies during spindle pole initiation in the green alga *Spermatozopsis similis*. *Protist 150*, 163–181.
57. Weber, C., Lee, V. D., Chazin, W. J., and Huang, B. (1994) High level expression in *Escherichia coli* and characterization of the EF-hand calcium-binding protein caltractin. *J. Biol. Chem. 269*, 15795–15802.
58. Barbato, G., Ikura, M., Kay, L. E., Pastor, R. W., and Bax, A. (1992) Backbone dynamics of calmodulin studied by ^{15}N relaxation using inverse detected two-dimensional NMR spectroscopy: The central helix is flexible. *Biochemistry 31*, 5269–5278.
59. Martinez-Sanz, J., Kateb, F., Assairi, L., Blouquit, Y., Abergel, D., Bodenhausen, G., Mouawad, L., and Craescu, C. T. (2010) Structure, dynamics, and thermodynamics of the human centrin 2/hSfi1 complex. *J. Mol. Biol. 395*, 191–204.
60. Black, D. J., Tikunova, S. B., Johnson, J. D., and Davis, J. P. (2000) Acid pairs increase the N-terminal Ca^{2+} affinity of CaM by increasing the rate of Ca^{2+} association. *Biochemistry 39*, 13831–13837.
61. Strynadka, N. C., and James, M. N. G. (1989) Crystal structures of the helix-loop-helix calcium-binding proteins. *Annu. Rev. Biochem. 58*, 951–991.
62. Salisbury, J. L. (2008) Breaking the ties that bind centriole numbers. *Nat. Cell Biol. 10*, 255–257.